

Research Article

Studies of dose distribution to Lung and Stomach and Estimation of Second Cancer Risk due to Outfield Dose in Radiotherapy with ⁶⁰Co Teletherapy Beam

MZ Hossain¹, MUH Musfika², N Arobi^{2,3}, T Siddiqua³, HM Jamil³, AKM Moinul Haque Meaze¹ and Md Shakilur Rahman^{3*}

¹Department of Physics, University of Chittagong, Chattogram-4331, Bangladesh

²Department of Physics, Jahangirnagar University, Savar, Dhaka-1342, Bangladesh

³Secondary Standard Dosimetry Laboratory, Bangladesh Atomic Energy Commission, Savar, Dhaka-1349, Bangladesh

Abstract

A critical component of the radiation regimen for treating cancer patients is the precise dose delivery to the treatment organ while minimizing the dose to the healthy tissue. This study aims to evaluate in-field organ dose and dose distribution outside the target organs to estimate the excess lifetime risk of second cancer. The study was carried out with a male Alderson Rando Phantom. 20 sets of thermoluminescence dosimeters (MTS-100) were used in this study. The in-field organs absorbed dose was measured by inserting TLDs at different geometrical depths of the left lung, right lung, and stomach, and for peripheral organs skin dose TLDs were placed at the surface of the corresponding organs. Target organs were irradiated at 100 cGy and 200 cGy by a ⁶⁰Co teletherapy unit, and irradiated TLDs were read out by a RE-2000 TLD reader. For precise dose delivery to the cancerous organs by ⁶⁰Co teletherapy, the depth dose correction factor for lung cancer treatment is 0.8667 ± 0.01 , and for the stomach is 0.7856 ± 0.017 . In the case of the treatment for the lung and stomach, the closest organs received significant doses compared to the other distant organs. Thus, the risk of second cancer due to the peripheral dose is obtained. The stomach is at the highest risk when the lung is the target and the liver is at the highest risk when the stomach is the targeted organ.

Introduction

About 10 million deaths occurred due to cancer in 2020 and it is regarded as the second greatest cause of mortality worldwide. External beam radiation is recommended for roughly 50% - 70% of cancer patients in addition to other forms of treatment like surgery and chemotherapy [1-4].

The central goal of radiotherapy is to destroy all tumor cells while causing as little harm as possible to the surrounding healthy cells, therefore the therapeutic dose is prescribed based on a number of parameters including the type, size, location, and staging of the lesion [1]. Radiation therapy is effective if the tumor receives only the prescribed dose. This necessitates precision in dose delivery of at least 3.5%, as recommended

by the International Commission on Radiological Protection [5]. Patients with primary cancers who undergo radiation therapy may develop second cancers in tissues and organs due to the outfield dose that was intended to be irradiated [6]. Within a treatment field, primary radiation is responsible for the majority of the high radiation doses experienced by inside organs. The doses gradually decrease and are primarily ascribed to stray radiation as the distance from the treatment field grows and the organs get more distant from the treatment field [7-10]. Secondary radiation sources such as photon leakage through the treatment head of the accelerator (known as "head leakage") scattered radiation from collimators, beam modifiers, and internal patient scatter contribute to the small amount of stray radiation that reaches the patient outside of

More Information

***Address for correspondence:**

Md Shakilur Rahman, Secondary Standard Dosimetry Laboratory, Bangladesh Atomic Energy Commission, Savar, Dhaka-1349, Bangladesh, Email: shakilurssdl@baec.gov.bd

Submitted: July 22, 2023

Approved: August 07, 2023

Published: August 08, 2023

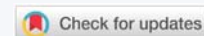
How to cite this article: Hossain MZ, Musfika MUH, Arobi N, Siddiqua T, Jamil HM, et al. Studies of dose distribution to Lung and Stomach and Estimation of Second Cancer Risk due to Outfield Dose in Radiotherapy with ⁶⁰Co Teletherapy Beam. Int J Phys Res Appl. 2023; 6: 136-143.

DOI: 10.29328/journal.ijpra.1001063

Copyright license: © 2023 Hossain MZ, et al.

This is an open access article distributed under the Creative Commons Attribution License, which permits unrestricted use, distribution, and reproduction in any medium, provided the original work is properly cited.

Keywords: Radiotherapy; Alderson rando phantom; Thermoluminescence dosimeter; Outfield dose; Second cancer risk



the primary field [11-13]. In experiments, it was discovered that the dose scattered from the patient's body is the primary source of dosage close to the field edge, while leakage radiation is responsible for the outfield dose at a farther distance from the field edge [14]. Stray radiation doses are unavoidable and, in some situations, non-negligible, despite the fact that they are modest in comparison to therapeutic levels. The severity of deterministic effects, such as cataractogenesis and the danger of stochastic consequences, such as radiogenic cancer, are both increased by exposure to stray radiation [12,15]. According to Diallo et al., a significant proportion of second malignancies (22%) developed in remote areas beyond the treatment field, while the bulk of cancers (66%) develop in the margin of the irradiated region or the "beam-bordering" zone that is the closest to the target organ. In the field areas, fewer cases of second cancer (12%) develop [16]. The lifetime risk of a second cancer is strongly correlated with patient age, and it is more likely to occur in the organs that are closest to the target volume than in remote out-of-field organs. Because of enhanced radiosensitivity, younger individuals were at higher risk than older ones [17-21]. Knowledge of both primary and stray radiation is necessary for estimating the arisen risk to organs such as second cancer risk [22]. Radiotherapy Treatment Planning Systems (TPS) are not intended to be used for out-of-field dosage estimations. Dose estimations using TPSs are known to be poor, especially for out-of-field areas [23-26]. The potential for calculating the risk of second cancer from out-of-field doses has sparked renewed interest in this area of research. Several new types of research highlight the significance of accurate dosage monitoring. Out-of-field exposure for photons (X-rays) increases with increasing beam energy due to the creation of biologically hazardous neutrons, and this dose is substantially larger for photons than for carbon ions [24]. The research showed that the out-of-field dosage was often underestimated by the treatment planning system by 40% - 50% and that this underestimating deteriorated with increasing distance from the field boundary [2,7,8].

The goal of the current investigation was to determine how much radiation should be delivered to the target tissues at various depths using the conventional ^{60}Co source approach.

Methods and materials

The study fulfilled two major parts- (a) calibration of thermoluminescence dosimeters (TLDs) and (b) measuring the target organ doses and the skin dose of peripheral organs of Alderson rando phantom using the calibrated TLDs.

The experimental measurements were performed by using a male anthropomorphic Alderson Rando phantom (Phantom Laboratory, Salem, New York) and LiF: Mg, Ti thermoluminescence dosimeters (MTS-100, Mirion technology, Germany) for dose measurement. These chips are of size 4.5 mm in diameter and 0.9 mm in thickness and are

irradiated by a known gamma source ^{60}Co teletherapy unit (Best Theratronics, Ottawa, Ontario, Canada).

Calibration of TLD

TLDs have been calibrated in the air for low dose levels and in tissue equivalent water phantom for high dose levels following the IAEA calibration formalism [27,28]. TLDs have been calibrated on the skin surface of the Alderson Rando phantom to measure the Entrance Surface Dose (ESD) of outfield organs of the Rando phantom. Initially, calibration was carried out in the air for low dose levels [27,28]. In this method, dosimetry of 20 sets of TLDs was carried out in the air on the skin of Alderson rando phantom and was exposed by ^{137}Cs source to 1, 2, 3, 4, 5, 10, and 20 mSv dose. TLDs were read out by a RE-2000 TLD Reader (RE-2000, Mirion technology, Germany).

Again, to measure the organ dose of Alderson rando phantom at different depths, TLDs have been calibrated in tissue equivalent water phantom using a ^{60}Co teletherapy beam [27,28]. Reference dosimetry was done in IAEA water phantom (300 × 300 × 300 mm, wall thickness is 15mm) using IBA FC65-G Farmer chamber (0.65 cm³) in the reference condition (field size: 10 × 10 cm², SSD: 100 cm, Chamber at depth: 5 cm). TLDs were set in a plastic plate hole, and covered by latex to ensure the TLD plate was waterproof. Finally, TLDs were irradiated ^{60}Co beams following the reference dosimetry for 50 cGy, 100 cGy, 150 cGy, and 200 cGy. The calibration factor of individual TLD was determined for each dose level.

Dose measurement

To measure the target organ dose and skin dose of corresponding peripheral organs of AR phantom were performed for the lung (left lung & right lung) and stomach. The phantom is transacted horizontally into 2.5 cm thick slices having a total of 36 slices. Each slice has holes plugged with bone, soft-tissue, or lung-tissue equivalent pins which could be replaced by TLDs. When the left and right lungs were the target organs, a central lung slice (phantom slice #16) was chosen as the target slice (Figure 1). And in the case of the stomach, two middle slices of the stomach (slice no. 20 and 21) were chosen as targeted slices (Figure 2). For dose distribution of target organs, TLD was placed in the defined slice of target organs at different depths to measure the distribution of in-field targeted organ dose and to compare the dose with the standard dose.

Other TLDs were placed on the surface of defined organs of Alderson Rando phantom for out-of-field dose. After positioning the TLDs in specified geometry, each target organ was irradiated separately by ^{60}Co teletherapy unit at 100 cGy and 200 cGy doses at reference 10 × 10 cm² field size (Figure 3). The target organs absorbed dose at different depths is calculated for each dose level by [29].



Figure 1: Inner view of lung targeted slice of Alderson rando phantom with TLDs.

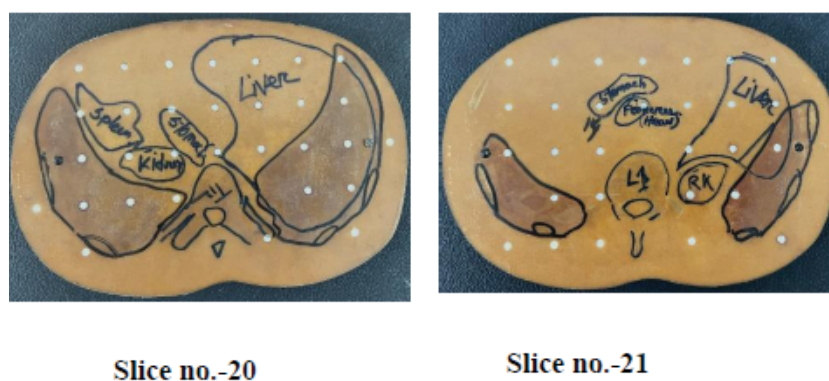


Figure 2: Inner view of stomach targeted slice of Alderson rando phantom with TLDs.



Figure 3: Irradiation of Alderson Rando phantom by ⁶⁰Co Teletherapy unit.

$$\text{Absorbed dose} = \text{TLD response dose} \times \text{TLD calibration factor}$$

The peripheral entrance surface dose of respective organs was calculated by multiplying the TLD response dose by the corresponding TLD calibration factor after the irradiation of the Alderson rando phantom by 100 cGy and 100 cGy.

Results and discussions

Figure 4 shows the variation of crystal sensitivity of 20 sets

of TLDs at 2 mSv exposures by the ¹³⁷Cs source in the same manner as the calibration process in the air. The uncertainty of the variation of crystal sensitivity of our TLDs is 0.21%. Again, Figure 5(a) shows the dose-response curve of TLDs in water for 50 cGy, 100 cGy, 150 cGy and 200 cGy doses have an uncertainty of 1.976% within the recommended limit of 3% - 5% [30]. Figure 5(b) shows the calibration curve of TLD-100 in the air for 1, 2, 3, 4, 5, 10, and 20 mSv dose levels. It was found that dose-response linearity is very close to unity having an uncertainty of 1.04%.

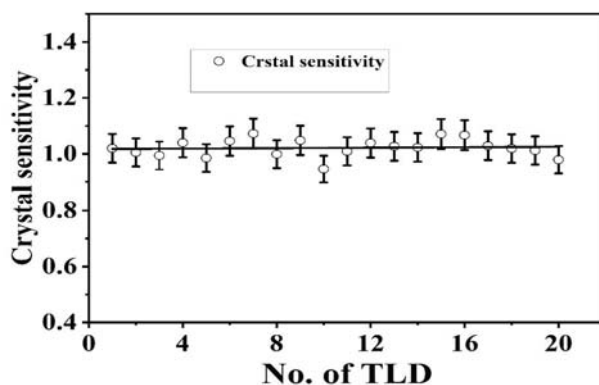


Figure 4: Variation of crystal sensitivity of each TLD.

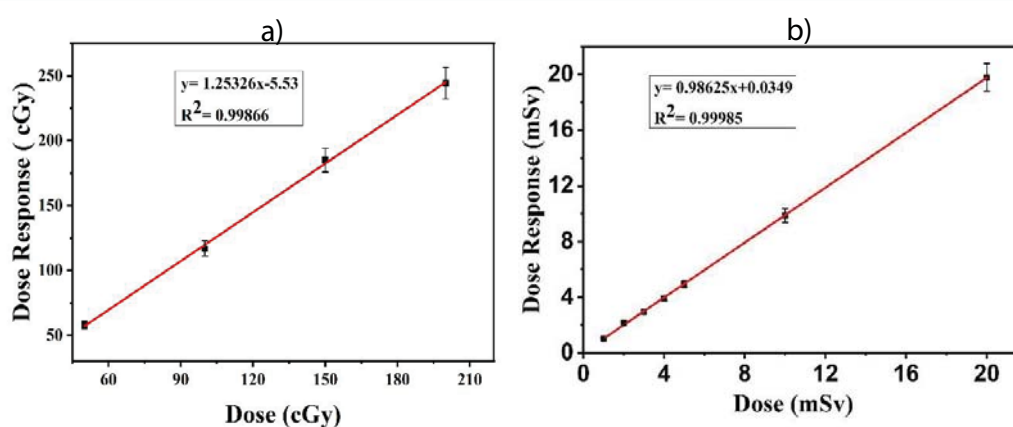


Figure 5: (a) Calibration curve of TLD when exposed to water at ^{60}Co teletherapy beam and (b) calibration curve of TLD when exposed to air at ^{137}Cs .

Comparison between measured and calculated value of target organs absorbed dose at different depths

The dose distribution of target organs (lung) at different depths was measured by inserting the TLDs at 15, 16 & 17 slices of the left, and right lung, and for the measurement of dose distribution of stomach at different depths, TLDs were placed at 20 & 21 no. slices of Alderson rando phantom for 10 cm \times 10 cm field size. The measured dose was compared with central axis depth dose data for 10 cm \times 10 cm field size using a ^{60}Co beam [31]. Figures 6-8 show that the dose at the target organ (left lung, right lung & stomach) is the function of the depth. The dose decreased with the increase in the depth value. The TLD-measured dose is always less than the calculated standard dose. Figures 6-8 show the variations of absorbed dose with depth when both the lungs and stomach are irradiated at 100 cGy and 200 cGy doses and this study reveals that; the measured dose is lower than the calculated standard dose for both lungs and stomach. The ratio of the measured dose and the standard dose is (0.75 - 0.96) for the left lung and (0.84 - 0.90) for the right lung which are close to 1. The study demonstrates that the depth dose correction factors for the treatment of the left lung and right lung using ^{60}Co beam are 0.8567 ± 0.0225 and 0.8768 ± 0.0072 respectively. The study carried that the depth dose correction factor is 0.8667 ± 0.01 for lung treatment using a ^{60}Co teletherapy unit. The ratio of

the measured dose and the calculated dose lies between (0.6 - 0.88) for the stomach. The study demonstrated that the depth dose correction factor using a ^{60}Co teletherapy beam for the treatment of the stomach is 0.7856 ± 0.017 .

Figures 6-8 show that, almost in every case, the measured dose is lower than the calculated. This underestimation of the measured dose might be due to the higher scattering of the photon beam [11,13,20]. The standard value is calculated using tissue equivalent material but the human body is rich in water molecules due to which a deviation is observed in the comparison Figures. But the ratio of the measured dose and the calculated dose is close to unity. This underestimation of the measured dose might be due to the higher scattering of the photon beam [11,13,20].

The pattern of underestimation of absorbed dose at different depths is not the same. Since Figure 1 shows that the sensitivity of all the TLDs is not the same and few TLDs are more sensitive to photon irradiation. These dosimeters show higher doses than the other dosimeters. Due to this inhomogeneity of crystal sensitivity of TLDs, the absorbed dose pattern might not be the same at different depths in three different cases. The study shows that the lung tissue absorbed higher radiation than the other target organs' stomach. Since the lung cavity is full of air, which has a lower density (0.3 g/cm^3) than the normal tissue, it received a higher dose [32].

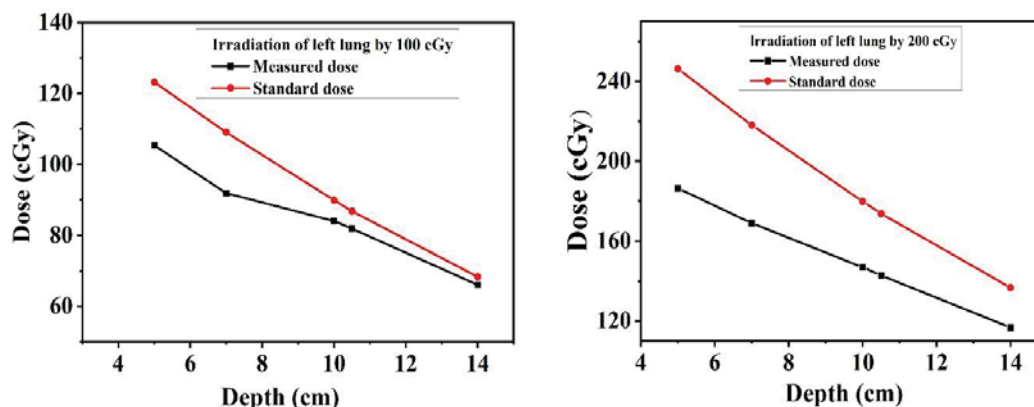


Figure 6: TLD dose and the calculated dose as a function of depth for the left lung.

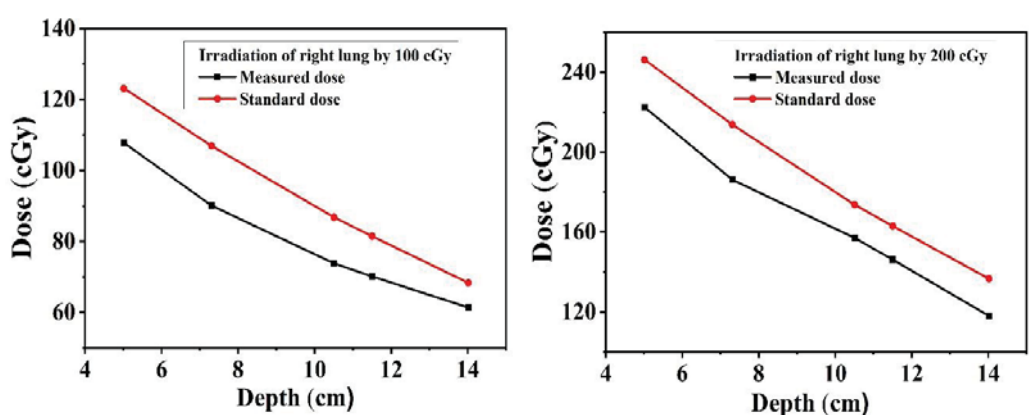


Figure 7: TLD dose and the calculated dose as a function of depth for the right lung.

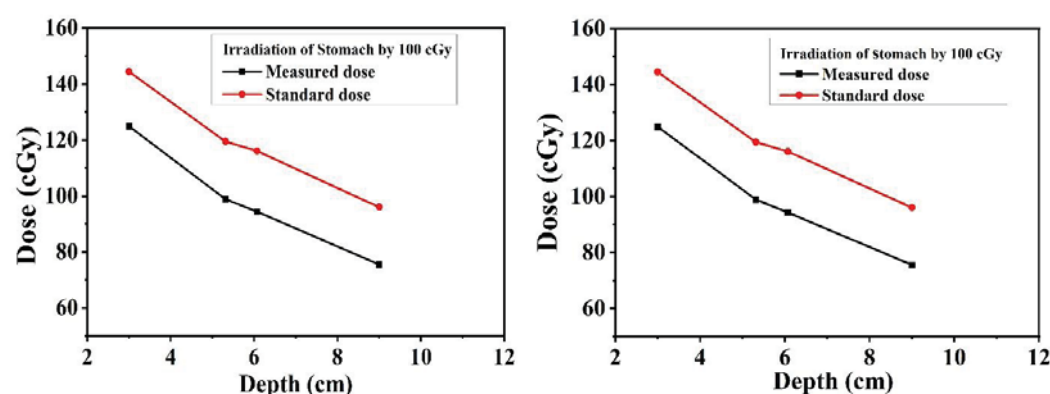


Figure 8: TLD dose and the calculated dose as a function of depth for the stomach.

Measurement of field organs entrance surface dose

Tables 1-3 represent ESD received by the outfield organs when the left lung, right lung, and stomach respectively are irradiated at 100 cGy, 200 cGy dose by ^{60}Co teletherapy unit. In the case of lung irradiation, the other parts of the lung and the closest organs of the lung: liver, colon, stomach, and thyroid received a significant amount of radiation than the distant organs. In the case of stomach irradiation, the dose received by the closer organs, lung, liver, kidney, and colon is significant as compared to the distant organs eye, and thyroid.

The outfield dose is the highest in the stomach when the lung is the targeted organ. As the left lung is nearer to the stomach than the right lung, ESD for the stomach is greater due to the left lung than the right lung. In this study, the dose distribution of different targets was investigated for the purposes of accurate dose delivery to the cancerous organs using traditional radiotherapy technique and considering the importance of second cancer risk estimation in out-of-field organs in patients who have radiation therapy treatment, the outfield dose of non-target organs was measured.



Table 1: Entrance surface dose received by the outfield organs for the target organ left lung.

Slice No. of phantom	Organs	Entrance surface dose (cGy)	
		For 100 cGy irradiation	For 200 cGy irradiation
4	Left Eye	2.10	2.30
4	Right eye	1.71	2.04
10,11	Thyroid	14.16	20.62
16	Right Lung	44.52	62.03
20	Stomach	65.62	96.60
20	Liver	15.48	20.53
20,21	Spleen, Left Kidney	5.42	7.95
22,23	Pancreas	2.47	3.28
28	Colon	24.63	33.12
32	Urinary Bladder	6.94	6.78

Table 2: Entrance surface dose received by the out-of-field organs for the target organ's right lung.

Slice No. of phantom	Organs	Entrance surface dose (cGy)	
		100 cGy	200 cGy
4	Left Eye	1.53	1.48
4	Right eye	1.14	1.96
10,11	Thyroid	10.87	18.96
16	Left Lung	31.60	48.94
20	Stomach	34.50	59.21
20	Liver	19.28	34.64
20,21	Spleen, Left Kidney	2.37	3.25
22,23	Pancreas	2.75	4.58
28	Colon	17.59	25.46
32	Urinary Bladder	4.27	5.13

Table 3: Entrance surface dose received by the out-of-field organs for the target organ stomach.

Slice No. of phantom	Organs	Entrance surface dose (cGy)	
		100 cGy	200 cGy
4	Left Eye	0.80	0.92
4	Right Eye	0.72	1.01
10,11	Thyroid	5.95	9.72
16	Right lung	33.15	53.13
16	Left lung	40.69	64.29
20	Liver	34.29	96.35
23	Right kidney	6.40	13.57
23	Left kidney	11.23	14.77
28	Colon	31.38	51.46
32	Urinary Bladder	4.93	07.32

Table 4: Estimating the risk of second cancer for 200 cGy.

Target Organ	Highest Dose Received by organ	Peripheral Dose(mSv) for 200 cGy	Estimated Risk Factor ($\times 10^{-3}$)
Left Lung	Stomach	96.60	139.1
Right Lung	Stomach	59.21	85.6
Stomach	Liver	96.35	138.7

Second cancer risk estimation

The Linear No-Threshold (LNT) model describes a relationship between the risk of harmful effects and the amount of exposure to ionizing radiation. The cancer risk coefficient predicted from the LNT model is 4.8×10^{-4} per rem [33]. Conventionally fractionated radiotherapy regimens are 4500 cGy to 6000 cGy given in 180 cGy to 200 cGy daily fractions, over five to six weeks [34-38]. To consider the highest possible risk of second cancer, the highest ESD is used for the risk estimation for the delivered dose of 200 cGy. Table

4 shows the risk estimation of second cancer for the delivered dose of 200 cGy.

Conclusion

We calculated the depth dose correction factor for the ⁶⁰Co teletherapy unit and assessed the dose distribution at several target organs, including the left lung, right lung, and stomach, kidney. This might be beneficial for delivering a precise dosage to malignant cells. Due to the scattering of the delivered beam, a less amount of dose than the prescribed reach to the target area, and this undue radiation is absorbed by the organs margined to the irradiated region. It demonstrated that; for accurate treatment and precise dose delivery to the cancerous organs by ⁶⁰Co teletherapy a depth dose correction factor is needed. The study also calculates the entrance surface dose for outfield organs and late consequences in healthy tissue in the future i.e. the risk of second cancer using the LNT model. As expected, our study results that the organs (liver, colon, stomach, thyroid for lung irradiation and lung, liver, kidney, and colon for stomach irradiation) closest to the target area received a significant amount of higher radiation than the distant organs. These organs also had a greater lifetime chance of developing a second cancer. The estimated risk factors are 139.1×10^{-3} , 85.6×10^{-3} and 138.7×10^{-3} when the left lung, right lung, and stomach were irradiated by 200 cGy respectively. To reduce excessive radiation when treating one portion of the lung, a shielding approach should be used in the remaining portion of the lung. Additionally, the kidney, pancreas, and other nearby organs should be protected while treating the stomach. The shielding technique should be used on delicate organs as well, such as the eyes. In impoverished nations like Bangladesh, ⁶⁰Co teletherapy has shown to be the most effective kind of radiation treatment. Therefore, it will be crucial to investigate the precise dose delivery to the infield organs and to estimate the long-term danger associated with utilizing a ⁶⁰Co teletherapy beam. Our results can be of interest for the dose estimations delivered in healthy tissues outside the treatment field for the radiotherapy patient, as well as in studies exploring radiotherapy's long-term effects.

Author's statement

This submission complies with ethical guidelines and all authors contributed to this manuscript.

Declaration of competing interest

The authors declare that they have no known competing financial interests or personal relationships that could have appeared to influence the work reported in this paper.

Acknowledgment

This article is based on the data extracted from a M.S. thesis dissertation presented to the Department of Physics, University of Chittagong. The authors would like to thank Secondary Standard Dosimetry Laboratory, Bangladesh Atomic Energy Commission for their sincere co-operation without which completion of this work was not easily possible.



References

1. Sant' A. Dose distribution in healthy tissues by computer modeling of the Alderson Rando phantom in Monte Carlo method. 2019.
2. Bahreyni Toossi MT, Soleymanifard S, Farhood B, Mohebbi S, Davenport D. Assessment of accuracy of out-of-field dose calculations by TiGRT treatment planning system in radiotherapy. *J Cancer Res Ther.* 2018 Apr-Jun;14(3):634-639. doi: 10.4103/0973-1482.176423. PMID: 29893331.
3. <https://www.who.int/news-room/fact-sheets/detail/cancer>
4. Baskar R, Lee KA, Yeo R, Yeoh KW. Cancer and radiation therapy: current advances and future directions. *Int J Med Sci.* 2012;9(3):193-9. doi: 10.7150/ijms.3635. Epub 2012 Feb 27. PMID: 22408567; PMCID: PMC3298009.
5. International Atomic Energy Agency. TRS-398, Absorbed dose determination in external beam radiotherapy: an international code of practice for dosimetry based on standards of absorbed dose to water. Vienna: IAEA; 2000.
6. Kry SF, Bednarz B, Howell RM, Dauer L, Followill D, Klein E, Paganetti H, Wang B, Wu CS, George Xu X. AAPM TG 158: Measurement and calculation of doses outside the treated volume from external-beam radiation therapy. *Med Phys.* 2017 Oct;44(10):e391-e429. doi: 10.1002/mp.12462. Epub 2017 Aug 20. PMID: 28688159.
7. Howell RM, Scarboro SB, Taddei PJ, Krishnan S, Kry SF, Newhauser WD. Methodology for determining doses to in-field, out-of-field and partially in-field organs for late effects studies in photon radiotherapy. *Phys Med Biol.* 2010 Dec 7;55(23):7009-23. doi: 10.1088/0031-9155/55/23/S04. Epub 2010 Nov 12. PMID: 21076193; PMCID: PMC3001332.
8. Huang JY, Followill DS, Wang XA, Kry SF. Accuracy and sources of error of out-of field dose calculations by a commercial treatment planning system for intensity-modulated radiation therapy treatments. *J Appl Clin Med Phys.* 2013 Mar 4;14(2):4139. doi: 10.1120/jacmp.v14i2.4139. PMID: 23470942; PMCID: PMC5714363.
9. Bahreyni Toossi MT, Soleymanifard S, Farhood B, Mohebbi S, Davenport D. Assessment of accuracy of out-of-field dose calculations by TiGRT treatment planning system in radiotherapy. *J Cancer Res Ther.* 2018 Apr-Jun;14(3):634-639. doi: 10.4103/0973-1482.176423. PMID: 29893331.
10. Alabdoaburas MM, Mege JP, Chavaudra J, Bezin JV, Veres A, de Vathaire F, Lefkopoulos D, Diallo I. Experimental assessment of out-of-field dose components in high energy electron beams used in external beam radiotherapy. *J Appl Clin Med Phys.* 2015 Nov 8;16(6):435-448. doi: 10.1120/jacmp.v16i6.5616. PMID: 26699572; PMCID: PMC5691002.
11. Huang JY, Followill DS, Wang XA, Kry SF. Accuracy and sources of error of out-of field dose calculations by a commercial treatment planning system for intensity-modulated radiation therapy treatments. *J Appl Clin Med Phys.* 2013 Mar 4;14(2):4139. doi: 10.1120/jacmp.v14i2.4139. PMID: 23470942; PMCID: PMC5714363.
12. Taddei PJ, Jalbout W, Howell RM, Khater N, Geara F, Homann K, Newhauser WD. Analytical model for out-of-field dose in photon craniospinal irradiation. *Phys Med Biol.* 2013 Nov 7;58(21):7463-79. doi: 10.1088/0031-9155/58/21/7463. Epub 2013 Oct 8. PMID: 24099782; PMCID: PMC4395760.
13. Benadjouad MA, Bezin J, Veres A, Lefkopoulos D, Chavaudra J, Bridier A, de Vathaire F, Diallo I. A multi-plane source model for out-of-field head scatter dose calculations in external beam photon therapy. *Phys Med Biol.* 2012 Nov 21;57(22):7725-39. doi: 10.1088/0031-9155/57/22/7725. Epub 2012 Nov 2. PMID: 23123826.
14. Kase KR, Svensson GK, Wolbarst AB, Marks MA. Measurements of dose from secondary radiation outside a treatment field. *Int J Radiat Oncol Biol Phys.* 1983 Aug;9(8):1177-83. doi: 10.1016/0360-3016(83)90177-3. PMID: 6409854.
15. Kaderka R, Schardt D, Durante M, Berger T, Ramm U, Licher J, La Tessa C. Out-of-field dose measurements in a water phantom using different radiotherapy modalities. *Phys Med Biol.* 2012 Aug 21;57(16):5059-74. doi: 10.1088/0031-9155/57/16/5059. Epub 2012 Jul 27. PMID: 22836598.
16. Diallo I, Haddy N, Adjadj E, Samand A, Quiniou E, Chavaudra J, Alziar I, Perret N, Guérin S, Lefkopoulos D, de Vathaire F. Frequency distribution of second solid cancer locations in relation to the irradiated volume among 115 patients treated for childhood cancer. *Int J Radiat Oncol Biol Phys.* 2009 Jul 1;74(3):876-83. doi: 10.1016/j.ijrobp.2009.01.040. Epub 2009 Apr 20. PMID: 19386434.
17. Hemalatha A, Mayilvaganan A, Joan M, Chougule A, Kumar H. Out-Of-Field Dose Measurement and Second Cancer-Risk Estimation Following External Beam Radiotherapy and Brachytherapy for Cervical Cancer Treatment: A Phantom Study, Iran J Med Phys. 2020; 17. doi: 10.22038/ijmp.2019.38166.1491.
18. Suleiman SA, Qi Y, Chen Z, Xu XG. Monte carlo study of organ doses and related risk for cancer in Tanzania from scattered photons in cervical radiation treatment involving Co-60 source. *Phys Med.* 2019 Jun;62:13-19. doi: 10.1016/j.ejmp.2019.04.024. Epub 2019 May 4. PMID: 31153393.
19. Suleiman SA, Salum SK, Masoud AO, Kisukari JD, Mazunga M, Huo W. Monte Carlo simulation of non-target organ doses and radiation-induced secondary cancer risk in Tanzania from radiotherapy of nasopharyngeal by using Co-60 source, Radiation Physics and Chemistry. Jun, 2020; 171. doi: 10.1016/j.radphyschem.2020.108731.
20. Newhauser WD, Fontenot JD, Mahajan A, Kornguth D, Stovall M, Zheng Y, Taddei PJ, Mirkovic D, Mohan R, Cox JD, Woo S. The risk of developing a second cancer after receiving craniospinal proton irradiation. *Phys Med Biol.* 2009 Apr 21;54(8):2277-91. doi: 10.1088/0031-9155/54/8/002. Epub 2009 Mar 20. PMID: 19305036; PMCID: PMC4144016.
21. Trott KR. Special radiobiological features of second cancer risk after particle radiotherapy. *Phys Med.* 2017 Oct;42:221-227. doi: 10.1016/j.ejmp.2017.05.002. Epub 2017 Nov 2. PMID: 29103987.
22. Aspradakis MM, Morrison RH, Richmond ND, Steele A. Experimental verification of convolution/superposition photon dose calculations for radiotherapy treatment planning Institute of physics publishing physics in medicine Experimental verification of convolution/superposition photon dose calculations for radiotherapy treatment planning. 2003. <http://iopscience.iop.org/0031-9155/48/17/309>
23. Das IJ, Cheng CW, Watts RJ, Ahnesjö A, Gibbons J, Li XA, Lowenstein J, Mitra RK, Simon WE, Zhu TC; TG-106 of the Therapy Physics Committee of the AAPM. Accelerator beam data commissioning equipment and procedures: report of the TG-106 of the Therapy Physics Committee of the AAPM. *Med Phys.* 2008 Sep;35(9):4186-215. doi: 10.1118/1.2969070. PMID: 18841871.
24. Court LE, Ching D, Schofield D, Czermanska M, Allen AM. Evaluation of the dose calculation accuracy in intensity-modulated radiation therapy for mesothelioma, focusing on low doses to the contralateral lung. *J Appl Clin Med Phys.* 2009 Apr 28;10(2):34-42. doi: 10.1120/jacmp.v10i2.2850. PMID: 19458589; PMCID: PMC5720454.
25. Kaderka R, Schardt D, Durante M, Berger T, Ramm U, Licher J, La Tessa C. Out-of-field dose measurements in a water phantom using different radiotherapy modalities. *Phys Med Biol.* 2012 Aug 21;57(16):5059-74. doi: 10.1088/0031-9155/57/16/5059. Epub 2012 Jul 27. PMID: 22836598.
26. Radiation Risk Assessment Tool - Lifetime Cancer Risk from Ionizing Radiation. (n.d.). Radiation Risk Assessment Tool - Lifetime Cancer Risk from Ionizing Radiation. <https://rep.nci.nih.gov/radtrat>
27. International Atomic Energy Agency. Technical Reports Series No. 277, Absorbed dose determination in photon and electron beams. 2nd ed. Vienna: IAEA; 1997.
28. International Atomic Energy Agency. TRS-398, Absorbed dose



- determination in external beam radiotherapy: an international code of practice for dosimetry based on standards of absorbed dose to water. Vienna: IAEA; 2000.
29. Podgorsak EB. Radiation Oncology Physics: A Handbook for Teachers and Students.
30. Cember H, Johnson T. Introduction to Health Physics: Fourth Edition.
31. Icrp. Annals of the ICRP Published on behalf of the International Commission on Radiological Protection.
32. Berrington de Gonzalez A, Iulian Apostoaiei A, Veiga LH, Rajaraman P, Thomas BA, Owen Hoffman F, Gilbert E, Land C. RadRAT: a radiation risk assessment tool for lifetime cancer risk projection. *J Radiol Prot.* 2012 Sep;32(3):205-22. doi: 10.1088/0952-4746/32/3/205. Epub 2012 Jul 19. PMID: 22810503; PMCID: PMC3816370.
33. National Research Council (US) Board on Radiation Effects Research. Health Risks from Exposure to Low Levels of Ionizing Radiation: BEIR VII, Phase I, Letter Report (1998). Washington (DC): National Academies Press (US); 1998. PMID: 25077203.
34. Amols HI, Weinhaus MS, Reinstein LE. The variability of clinical thermoluminescent dosimetry systems: a multi-institutional study. *Med Phys.* 1987 Mar-Apr;14(2):291-5. doi: 10.1118/1.596140. PMID: 3587157.
35. British Institute of Radiology. Central Axis Depth Dose Data for Use in Radiotherapy: BJR Supplement 25,1996.
36. <https://itis.swiss/virtual-population/tissue-properties/database/density/>
37. James CS, Bateman TM. Radiation considerations for cardiac nuclear and computed tomography imaging. *Clinical Nuclear Cardiology.* Elsevier Inc (2010): 149-162.
38. Gersh JA, Best RC, Watts RJ. The clinical impact of detector choice for beam scanning. *J Appl Clin Med Phys.* 2014 Jul 8;15(4):4801. doi: 10.1120/jacmp.v15i4.4801. PMID: 25207408; PMCID: PMC5875504